

Synergistic effect of total ionizing dose on single-event gate rupture in SiC power MOSFETs

Rongxing Cao(曹荣幸), Kejia Wang(汪柯佳), Yang Meng(孟洋), Linhuan Li(李林欢), Lin Zhao(赵琳), Dan Han(韩丹), Yang Liu(刘洋), Shu Zheng(郑澍), Hongxia Li(李红霞), Yuqi Jiang(蒋煜琪), Xianghua Zeng(曾祥华), and Yuxiong Xue(薛玉雄)

Citation: Chin. Phys. B, 2023, 32 (**6**): 068502. DOI: 10.1088/1674-1056/acbde7
Journal homepage: http://cpb.iphy.ac.cn; http://iopscience.iop.org/cpb

What follows is a list of articles you may be interested in

Dynamic modeling of total ionizing dose-induced threshold voltage shifts in MOS devices

Guangbao Lu(陆广宝), Jun Liu(刘俊), Chuanguo Zhang(张传国), Yang Gao(高扬), and Yonggang Li(李永钢)
Chin. Phys. B, 2023, 32 (**1**): 018506. DOI: 10.1088/1674-1056/ac9fc4

Radiation effects of 50-MeV protons on PNP bipolar junction transistors

Yuan-Ting Huang(黄垣婷), Xiu-Hai Cui(崔秀海), Jian-Qun Yang(杨剑群), Tao Ying(应涛), Xue-Qiang Yu(余雪强), Lei Dong(董磊), Wei-Qi Li(李伟奇), and Xing-Ji Li(李兴冀)
Chin. Phys. B, 2022, 31 (**2**): 028502. DOI: 10.1088/1674-1056/ac1331

Influence of characteristics' measurement sequence on total ionizing dose effect in PDSOI nMOSFET

Xin Xie(解鑫), Da-Wei Bi(毕大伟), Zhi-Yuan Hu(胡志远), Hui-Long Zhu(朱慧龙), Meng-Ying Zhang(张梦映), Zheng-Xuan Zhang(张正选), Shi-Chang Zou(邹世昌)
Chin. Phys. B, 2018, 27 (**12**): 128501. DOI: 10.1088/1674-1056/27/12/128501

Synergistic effect of total ionizing dose on single event effect induced by pulsed laser microbeam on SiGe heterojunction bipolar transistor

Jin-Xin Zhang(张晋新), Hong-Xia Guo(郭红霞), Xiao-Yu Pan(潘霄宇), Qi Guo(郭旗), Feng-Qi Zhang(张凤祁), Juan Feng(冯娟), Xin Wang(王信), Yin Wei(魏莹), Xian-Xiang Wu(吴宪祥)
Chin. Phys. B, 2018, 27 (**10**): 108501. DOI: 10.1088/1674-1056/27/10/108501

Synergistic effects of total ionizing dose on single event upset sensitivity in static random access memory under proton irradiation

Xiao Yao (肖尧), Guo Hong-Xia (郭红霞), Zhang Feng-Qi (张凤祁), Zhao Wen (赵雯), Wang Yan-Ping (王燕萍), Zhang Ke-Ying (张科营), Ding Li-Li (丁李利), Fan Xue (范雪), Luo Yin-Hong (罗尹虹), Wang Yuan-Ming (王园明)
Chin. Phys. B, 2014, 23 (**11**): 118503. DOI: 10.1088/1674-1056/23/11/118503

Synergistic effect of total ionizing dose on single-event gate rupture in SiC power MOSFETs

Rongxing Cao(曹荣幸)[1,†], Kejia Wang(汪柯佳)[1,2], Yang Meng(孟洋)[1], Linhuan Li(李林欢)[2], Lin Zhao(赵琳)[3], Dan Han(韩丹)[1], Yang Liu(刘洋)[1], Shu Zheng(郑澍)[1], Hongxia Li(李红霞)[1], Yuqi Jiang(蒋煜琪)[4], Xianghua Zeng(曾祥华)[1], and Yuxiong Xue(薛玉雄)[1,‡]

[1] *College of Electrical, Energy and Power Engineering, Yangzhou University, Yangzhou* 225127, *China*
[2] *College of Physics Science and Technology, Yangzhou University, Yangzhou* 225002, *China*
[3] *Institute of Special Environments Physical Sciences, Harbin Institute of Technology, Shenzhen* 518055, *China*
[4] *College of Intelligent Manufacturing, Yangzhou Polytechnic Institute, Yangzhou* 225002, *China*

(Received 23 October 2022; revised manuscript received 4 January 2023; accepted manuscript online 22 February 2023)

The synergistic effect of total ionizing dose (TID) and single event gate rupture (SEGR) in SiC power metal–oxide–semiconductor field effect transistors (MOSFETs) is investigated via simulation. The device is found to be more sensitive to SEGR with TID increasing, especially at higher temperature. The microscopic mechanism is revealed to be the increased trapped charges induced by TID and subsequent enhancement of electric field intensity inside the oxide layer.

Keywords: SiC power MOSFET, total ionizing dose (TID), single event gate rupture (SEGR), synergistic effect, TCAD simulation

PACS: 85.30.Tv, 61.80.Az, 61.80.Jh **DOI:** 10.1088/1674-1056/acbde7

1. Introduction

SiC is an attractive wide-bandgap semiconductor material due to its properties of high breakdown field, high thermal conductivity, and high saturated electron drift velocity, etc.[1–3] With these advantages, SiC devices are expected to play an important role in power device applications at ground level and in space.[4–6] The particle irradiation during its applications in space will cause radiation effects on devices, resulting in performance degradation or even catastrophic failure.

In previous studies, total ion dose (TID) and single event effect (SEE) were usually studied separately.[7–9] The TID effect has been studied in terms of irradiation conditions, such as temperature[10–12] and gate bias.[13–15] It has been revealed that the TID effect is induced by the radiation-induced holes moving toward the SiC/SiO_2 interface and trapped by defects in the oxide near the interface. Single event gate rupture (SEGR)[16,17] is a catastrophic failure mode of SEE,[18–20] which can destroy the ability of the gate to regulate current flow from the source to the drain by permanently damaging the gate insulator.[21] Recently, some studies[22,23] focused on the TID effect on SEGR in Si vertical double-diffused metal–oxide–semiconductor field effect transistors (MOSFETs). Researchers have found that the charge trapping could enhance the localized electric field, resulting in SEGR at reduced applied bias. In comparison with Si-based devices, SiC devices have an enhanced TID hardness.[17] However, they are more sensitive to SEE.[24–26] To date, there are almost no investigations on how SEGR effects are affected by the foregoing TID damage in SiC MOSFET power devices, especially the intrinsic causes and microscopic mechanisms have not been revealed.

In this work, we perform the simulation of the synergistic effect of TID on SEGR in SiC MOSFET utilizing the Technology Computer Aided Design (TCAD) platform. The radiation dose-dependent behavior of SEGR at different ambient temperatures is investigated. Combined with the spatial distribution of trapped charges and electric field intensity in the device, the microscopic mechanism of the synergistic effect of TID and SEGR is revealed.

2. TCAD simulations

The TCAD simulations in this work can be divided into three steps: Firstly, the TID effect in a SiC MOSFET power device with different doses of 200 krad (Si), 500 krad (Si), and 800 krad (Si) is simulated. Secondly, the SEGR effect is simulated and the mechanism is discussed. Thirdly, the successive simulations of TID and SEGR are performed to investigate the synergistic effect of TID, SEGR, and its mechanism.

2.1. Electrical modeling of device

The SiC MOSFET device investigated in this paper has a typical cell structure[27–30] as shown in Fig. 1. The lateral width and height of the cell structure are both 15 μm. The

†Corresponding author. E-mail: rxcao@yzu.edu.cn
‡Corresponding author. E-mail: yxxue@yzu.edu.cn

© 2023 Chinese Physical Society and IOP Publishing Ltd

doping concentrations of the N^+ source and the P^+ source are 1×10^{18} cm^{-3} and 8×10^{19} cm^{-3}, respectively. Both the junction depths are 1.5 μm. The doping concentration of the P base region is 1×10^{17} cm^{-3} with a junction depth of 3 μm. The doping concentrations of the N drift region and N^+ substrate are 1×10^{16} cm^{-3} and 1×10^{19} cm^{-3}, respectively. The thicknesses of the gate oxide layer and the buffer layer are 0.06 μm and 0.1 μm, respectively. The other dimensions of the device are indicated in Fig. 1. The rated voltage of the device is 900 V, and the gate-source threshold voltage $V_{gs(th)}$ is about 6 V.

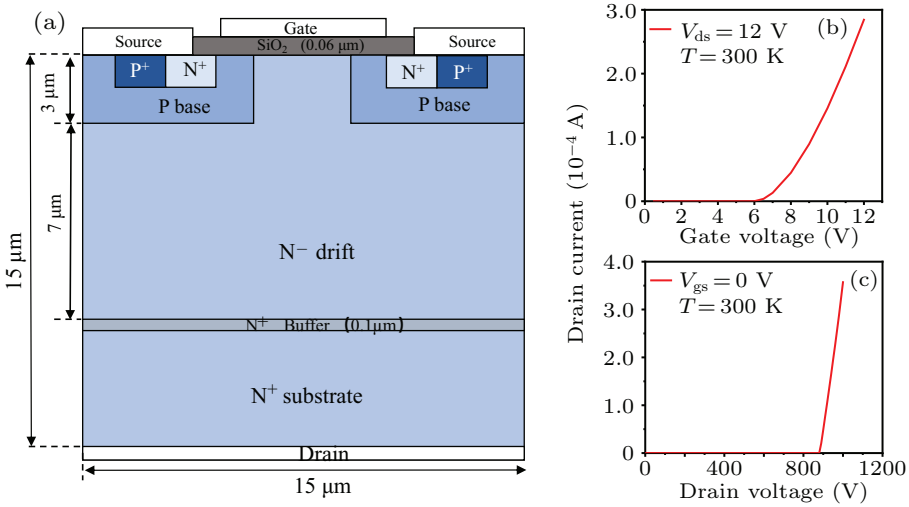


Fig. 1. Cross-sectional view of a vertical power SiC MOSFET cell.

2.2. Modeling of TID effect

Based on the electrical model, TID simulation was then performed by introducing oxide-trapped charges and interface-trapped charges in TCAD.[31] To simulate total dose effects in insulators, the oxide was converted to a semiconductor with the bandgap of SiO_2. Then the concentrations and characteristics of the bulk oxide and interface traps (e.g., energy level, capture cross-section) were initially defined in the oxide layer and the initial electron–hole density was defined to be approximately 1×10^{13} cm^{-3}–1×10^{15} cm^{-3}. After that, the SRH composite model,[32] Auger model,[33] CVT model,[34] Fermi–Dirac statistics model, band gap narrowing model, and bound-trap model were considered. Among them, the bound-trap model is specific for the TID effect, which enables modeling of traps coincident with ohmic boundaries. In TID simulation, the radiation-induced ionization, subsequent charge drift, and trapping in the oxide layer were simulated. The dose rate in the TID simulation was 50 rad(Si)/s and the total dose was used from 0 to 800 krad (Si). A positive gate-source voltage $V_{gs} = 10$ V was applied for a significant TID effect and the drain-source voltage was $V_{ds} = 0.05$ V.

2.3. Modeling of SEGR effect

Based on the above TID model, we replaced the bound-trap model in TID effect with impact ionization model to model the SEGR effect of the device. The device bias was chosen to be $V_{gs} = -5$ V, $V_{ds} = 55$ V to put the device in off-state. The LET value of the ion is 75 MeV·cm^2/mg. The heavy ions went perpendicularly into the sensitive JFET region, indicated by the black arrow in Fig. 2. The evolution of the electric field in gate oxide layer was simulated and the critical breakdown electric field of the oxide layer material (1×10^7 V/cm for SiO_2) was used to determine whether the SEGR occurs in the device.[9]

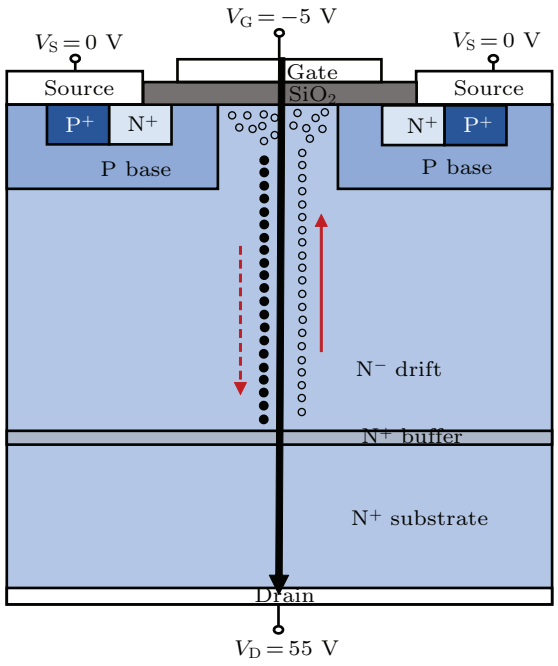


Fig. 2. Schematic of ion irradiation in SEGR modeling.

3. Results and discussion

3.1. Simulation analysis of TID effect

We have chosen a dose range of 0–800 krad (Si) to study the total dose effect of the device. In our study, we simulated

the total dose effect of a SiC MOSFET in steps of 100 krad (Si) and gave the variation of its threshold voltage with different total doses. In the text, as shown in Fig. 3, we selected three typical doses of 200 krad (Si), 500 krad (Si), and 800 krad (Si) to demonstrate the total dose effect of the device and to study its effect on SEGR. We note that the simulation findings for other doses are similar.

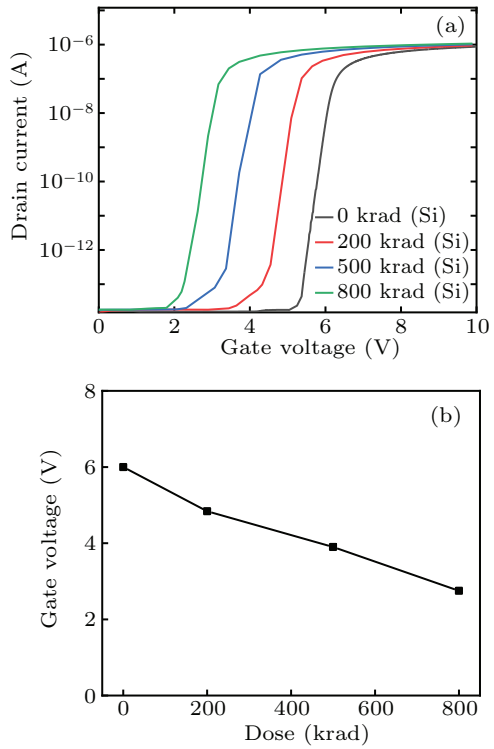


Fig. 3. Electrical characteristics of the device under different radiation doses at room temperature: (a) transfer characteristic under different doses, (b) threshold voltages under different doses.

As seen in Fig. 3(a), the transfer characteristic curve drifts negatively as the irradiation dose increases, while the transconductance remains unchanged. The threshold voltage decreases gradually from 6 V to 2.4 V with TID increasing, as shown in Fig. 3(b). These findings in TID simulation are consistent with the previously reported fact that the TID effect of vertical double-diffused MOSFETs (VDMOSs) comes mainly from the oxide-trapped charge contribution, which has no direct effect on the carrier drift and diffusion.[35]

3.2. Simulation analysis of SEGR effect

To compare the SEGR results with and without TID influence, solitary SEGR simulation was performed by ignoring the TID-induced oxide-trapped charge and interface-trapped charge.

The distribution of electron and hole concentration inside the device was derived from the SEGR simulation, as shown in Fig. 4. The electrons ionized by irradiated ions move along the incident path toward the drain driven by the electric field in the drift region since the gate is negatively biased and the drain is positively biased, as shown in Fig. 4(a). The ionized holes drift toward the gate due to positive drain bias, resulting in the accumulation of holes at the bottom of the gate oxide, as shown in Fig. 4(b). The conduction current is formed by the charge collection effect, causing a local short circuit between the drain and the interface SiC/SiO_2. Therefore, a large portion of the voltage is applied to the gate oxide layer, and the electric field of the oxide layer increases instantaneously, as shown in the inset of Fig. 4. If this electric field transient increment is large enough, the oxide layer near the incident track will be broken down. We note that there was no SEB observed in our simulation.

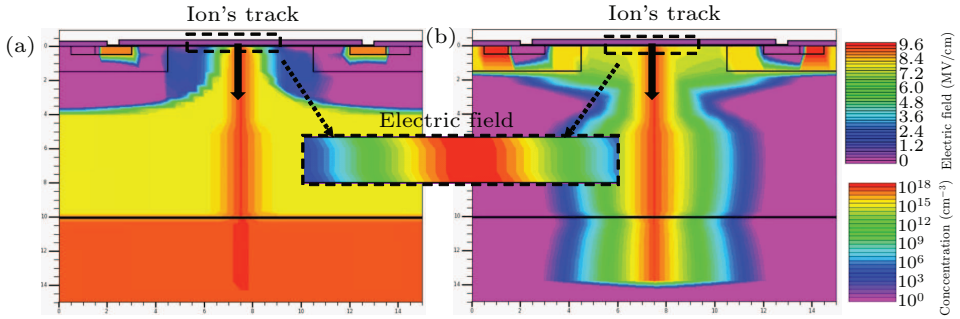


Fig. 4. The distribution of carrier concentration and electric field inside the gate oxide layer (inset) during SEGR: (a) electron concentration distribution, (b) hole concentration distribution.

3.3. Simulation analysis of TID effect on SEGR

Based on the solitary SEGR model, oxide-trapped charge and interface-trapped charge were introduced into the model for further SEGR simulations to investigate the effect of TID on SEGR.[36]

The spatial and temporal evolution of the electric field in the gate oxide layer for different doses was investigated. As shown in Fig. 5, the electric field in the oxide layer reaches a maximum at $t \approx 10$ ps. The maximum of the electric field increases with the increase of the total dose, from 9.8 MV/cm at 0 krad (Si) to 10.83 MV/cm at 800 krad (Si), as shown in the inset of Fig. 5. This finding demonstrates that the SiC device is more sensitive to SEGR when TID effect is introduced, which is similar to the previous experimental findings in Si

VDMOS.[22,23]

To reveal the mechanism of this synergistic effect of TID on SEGR, we firstly performed the simulation of the trapped charge distribution and electric field distribution in the oxide layer at different doses before heavy ion irradiation. Figure 6 shows that the charges are mainly trapped in the central region of the oxide layer, which is consistent with the previous reports that the oxide-trapped charge plays a dominant role in the TID effect of MOS devices.[22,37] Moreover, the concentration of trapped charges increases with the total doses, and the trapped holes have a much higher concentration than electrons.

Furthermore, we studied the spatial distribution of the electric field in the oxide layer at different irradiation doses. The field distribution is shown in Figs. 7(a)–7(d) when the bias is $V_{gs} = 5$ V before heavy ion irradiation. It can be found that the field intensity in the oxide layer becomes significantly larger with increasing the radiation dose. Figure 7(e) shows the comparison of the electric field intensity distribution in the oxide layer after different doses along the central track of the gate, i.e., the heavy ion's track. We can find that the electric field intensity in the oxide layer is not uniformly distributed, and the field intensity is higher near the gate/SiO_2 interface.

After that, as shown in Fig. 8, we further simulated the spatial distribution of the electric field when the device with different total doses was irradiated by heavy ions. From Figs. 8(a)–8(d), we can find that the electric field is not uniformly distributed in the oxide layer. The electric field intensity near the gate/SiO_2 interface is higher and increases with the total doses, which is similar to the results in solitary TID simulation.

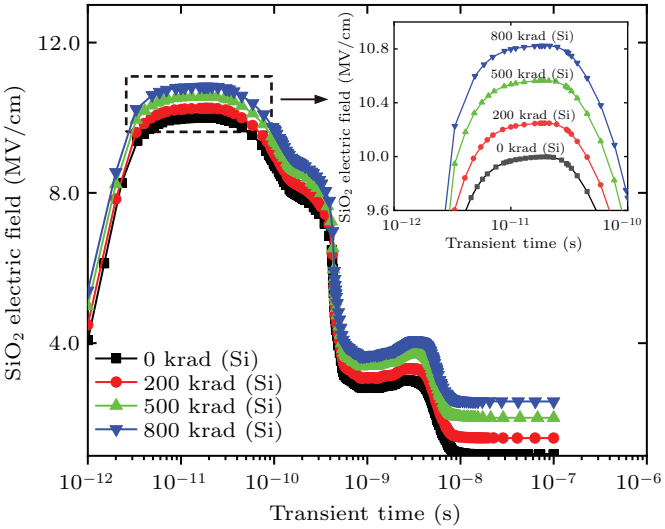


Fig. 5. The time evolution of the maximum electric field in the gate oxide layer at room temperature for different doses. The inset is the zoom-in of the peak region marked by the dotted box.

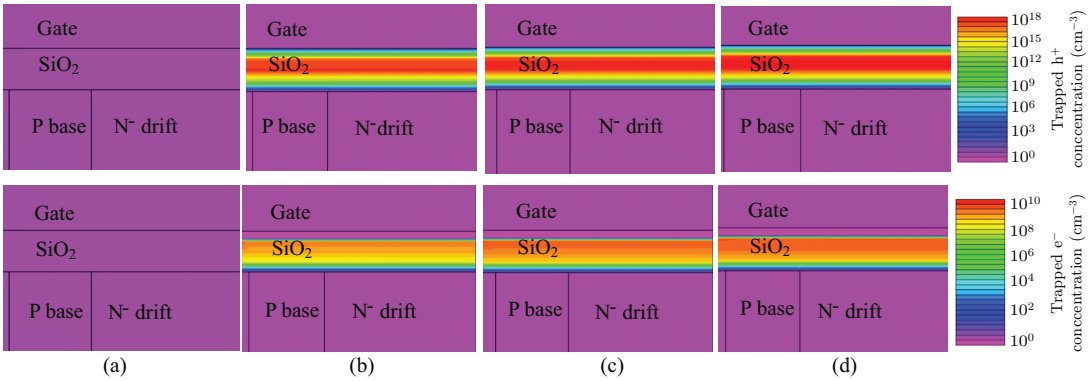


Fig. 6. Distribution of trapped charges in the gate oxide layer under different radiation doses: (a) 0 krad (Si), (b) 200 krad (Si), (c) 500 krad (Si), (d) 800 krad (Si). The top and bottom rows show the concentration of trapped holes and electrons, respectively.

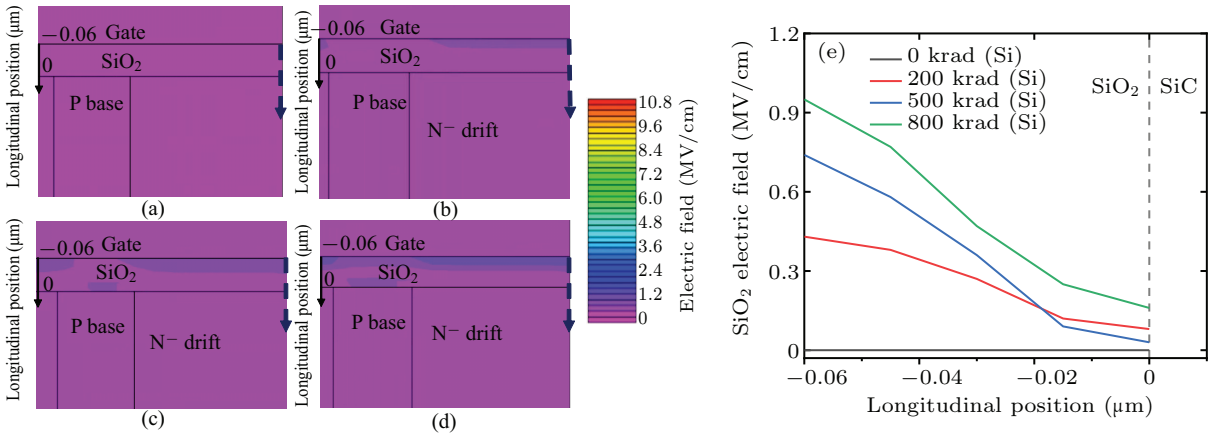


Fig. 7. Spatial distribution of electric field in the gate oxide layer after different radiation doses: (a) 0 krad (Si), (b) 200 krad (Si), (c) 500 krad (Si), (d) 800 krad (Si), (e) comparison of electric field distribution along the central track of gate as marked by the black dotted line in (a)–(d).

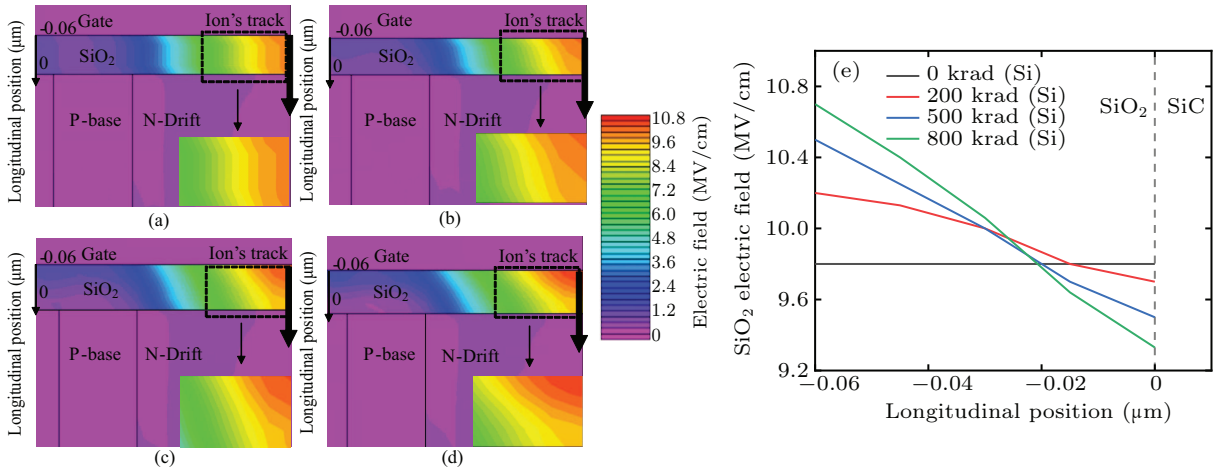


Fig. 8. Spatial distribution of the electric field when the device with different total doses is irradiated by heavy ions, (a) 0 krad (Si), (b) 200 krad (Si), (c) 500 krad (Si), (d) 800 krad (Si), (e) comparison of electric field distribution along the ion's track as marked by the black arrow.

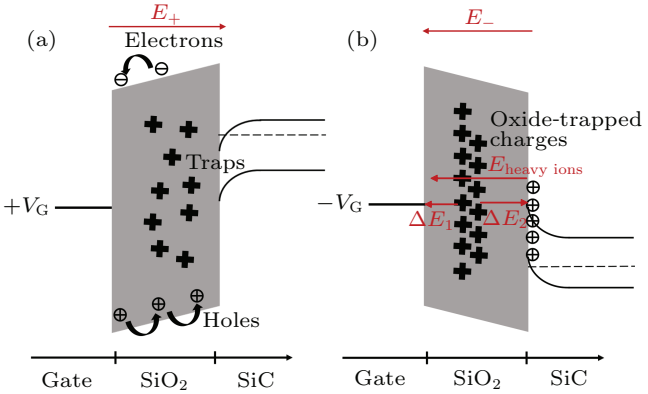


Fig. 9. Energy band diagram for MNOS structure during irradiation on the gate and corresponding electron–hole motion during TID (a) and after heavy ion irradiation (b).

In comparison with the spatial distribution of the field after the solitary TID effect shown in Fig. 7, we can see that after heavy ion irradiation, the electric field in the gate oxide layer increases significantly. For example, the electric field is 0.95 MV/cm under the radiation dose of 800 krad (Si) and increases up to 10.7 MV/cm after the incidence of ion. It can be seen from Fig. 8(e) that the spatial inhomogeneity of the electric field becomes greater with the increase of the radiation dose.

Then, we discuss the microscopic mechanism of the above findings in the synergistic effect investigation. As shown in Fig. 9(a), the gate voltage is positive and electron–hole pairs are generated in SiO_2 during total dose irradiation. The holes with lower mobility are trapped in the oxide layer during the transport process, forming oxide-trapped charges in the central region of the oxide layer. The trapped charges induced by TID could introduce additional electric fields $\Delta \boldsymbol{E}_1$ and $\Delta \boldsymbol{E}_2$ with different directions as shown in Fig. 9(b). These theoretical studies in the TID simulations are consistent with previous experimental findings in SiC devices.[13–15] Therefore, the field intensity is higher near the gate/SiO_2 interface since $\Delta \boldsymbol{E}_1$ is in the same direction as the field induced by the negatively biased gate before heavy ion irradiation, as shown in Fig. 7(e).

During the incidence of the heavy ions, a large number of electron–hole pairs are generated near the ion's track. The applied drain-source voltage makes the holes drift towards the SiC/ SiO_2 interface and accumulate there, resulting in the electric field ($\boldsymbol{E}_{\text{heavy_ions}}$) inside the oxide layer as shown in Fig. 9(b), which is consistent with the previous experiments.[17,24] The additional field near the gate/SiO_2 interface $\Delta \boldsymbol{E}_1$ has a direction as the same as $\boldsymbol{E}_{\text{heavy_ions}}$, so the superimposition of these two electric fields leads to the local field enhancement near the gate/SiO_2 interface, which is consistent with the results in Fig. 8(e). On the contrary, the direction of the additional field $\Delta \boldsymbol{E}_2$ near the SiC/SiO_2 interface is opposite to $\boldsymbol{E}_{\text{heavy_ions}}$, thus weakening the electric field on the SiC/ SiO_2 side. With the increase of the total ionizing dose, the additional fields ($\Delta \boldsymbol{E}_1$ and $\Delta \boldsymbol{E}_2$) become larger, resulting in the enhancement of the spatial inhomogeneity.

Therefore, the synergistic effect of TID and SEGR makes the electric field intensity in the oxide layer higher and the inhomogeneity of field distribution higher, which leads the device to be more sensitive to the SEGR effect.

3.4. The influence of temperature on synergy effect

Moreover, we study the influence of temperature on the synergistic effect. Figure 10(a) shows the time evolution of the maximum electric field in the gate oxide layer at 300 K and 400 K for two typical doses of 500 krad (Si) and 800 krad (Si) and subsequent heavy ion irradiation. The field in the oxide layer increases at high temperatures, e.g., it changes from 10.7 MV/cm at 300 K to 10.85 MV/cm at 400 K for the dose of 800 krad (Si) as shown by the blue curves in Fig. 10(a).

This temperature dependence can also be illustrated by the threshold voltage of the SEGR effect. The applied voltage is initially set to 45 V and ramps up with steps of 1 V. The breakdown criterion of SEGR simulation is 10 MV/cm

for SiO_2. As shown in Fig. 10(b), the SEGR threshold voltage decreases with the TID effect and has a reduction at high temperatures, e.g., it decreases from 50 V at 300 K to 48 V at 400 K under the dose of 800 krad (Si). These findings demonstrate that the SEGR will be more sensitive to the TID effect at high temperatures.

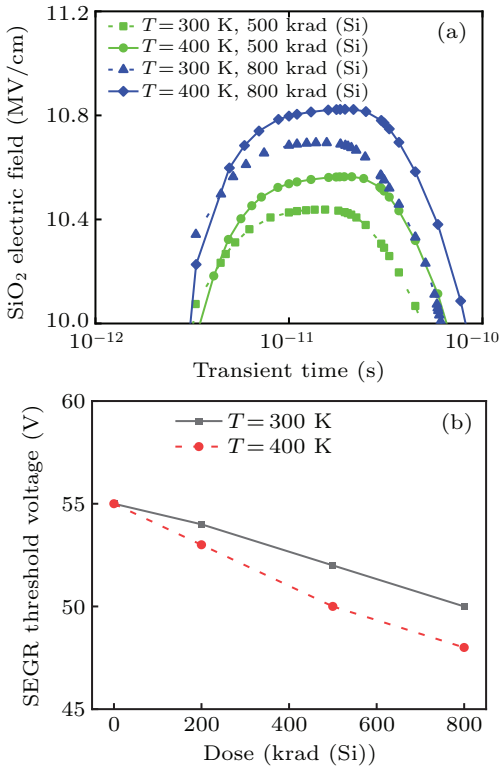


Fig. 10. The influence of temperature on the synergistic effect: (a) the time evolution of the maximum electric field in the gate oxide layer at different temperatures and doses, (b) the total dose-dependent SEGR threshold voltages at different temperatures.

To reveal the mechanism of the temperature dependence of the TID effect on SEGR, the solitary TID and SEGR at different temperatures were simulated, respectively. We performed the SEGR simulation without TID, and the evolution of electric field in the oxide layer at different temperatures is shown in Fig. 11(a). The maximum electric fields at 300 K and 400 K are nearly the same, indicating that the temperature has almost no influence on the SEGR effect in this temperature range.

Moreover, the solitary TID effect is simulated at different temperatures and the derived threshold voltages of SiC MOSFET under different doses are shown in Fig. 11(b). It can be found that the device has a lower threshold voltage at higher temperatures. The higher degradation of the threshold voltage can be attributed to the higher carrier mobility and the resultant increase of oxide-trapped charges at higher temperatures, which is consistent with previous reports.[8,38]

The electric fields in the oxide layer at different temperatures are compared in Fig. 12. It can be found that the spatial inhomogeneity of the field is higher at 400 K (solid curves)

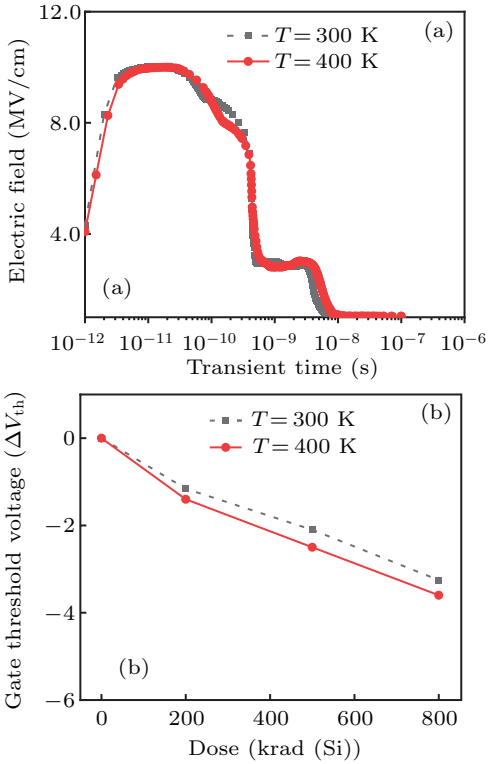


Fig. 11. Simulation of the solitary TID and SEGR effects at different temperatures: (a) comparison of the electric field in the gate oxide layer at different temperatures, (b) total ionizing dose-dependent threshold voltage of SiC MOSFETs at room temperature and 400 K.

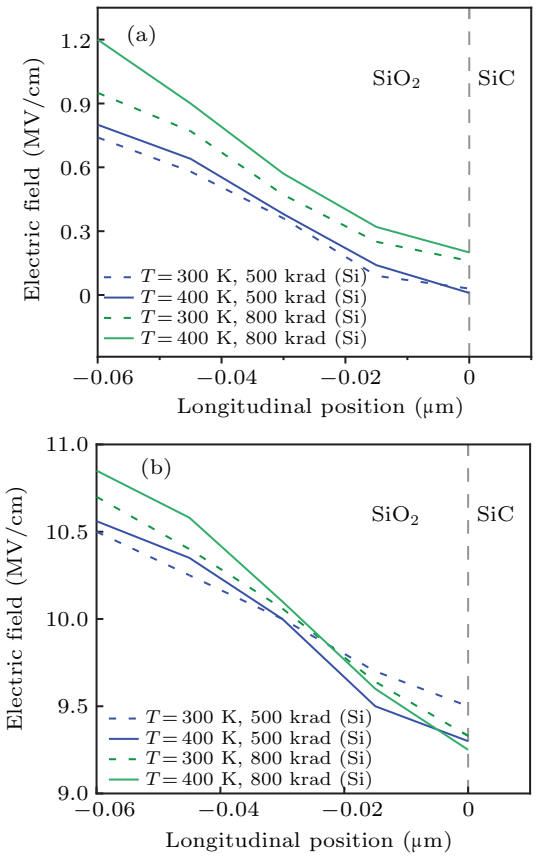


Fig. 12. Comparison of the electric field in the gate oxide layer at different temperatures before (a) and after (b) ion irradiation.

than that at 300 K (dashed curves) both before and after ion irradiation. Moreover, the field intensity near the gate/SiO_2

interface increases at high temperatures, and this increment is larger under higher total dose. Therefore, we can conclude that the mechanism of the more sensitive SEGR to TID effect at high temperature is the increased oxide-trapped charge and the resultant enhancement of local electric field, which confirms again the mechanism of synergistic effect of TID on SEGR revealed at room temperature.

4. Conclusions

In summary, we have investigated the synergistic effect of TID and SEGR in SiC power MOSFETs via TCAD simulation. It is found that the field intensity gets higher and the SEGR threshold voltage becomes lower with increasing total irradiation dose. The increased sensitivity in SEGR induced by TID can be attributed to the increased trapped charges induced by TID and the resultant enhancement of the local electric field inside the oxide layer. This microscopic mechanism is also confirmed by the further increase of SEGR sensitivity influenced by TID at higher temperature.

Acknowledgements

Project supported by the National Natural Science Foundation of China (Grant No. 12004329), Open Project of State Key Laboratory of Intense Pulsed Radiation Simulation and Effect (Grant No. SKLIPR2115), Postgraduate Research and Practice Innovation Program of Jiangsu Province (Grant No. SJCX22_1704), and Innovative Science and Technology Platform Project of Cooperation between Yangzhou City and Yangzhou University, China (Grant Nos. YZ202026301 and YZ202026306).

References

[1] Kimoto T and Yonezawa Y 2018 *Mater. Sci. Semiconduct. Process.* **78** 43
[2] Abbate C, Busatto G, Tedesco D, Sanseverino A, Silvestrin L, Velardi F and Wyss J 2019 *IEEE Trans. Electron. Devices* **66** 4235
[3] Hudgins J L, Simin G S, Santi E and Khan M A 2003 *IEEE Trans. Power Electron.* **18** 907
[4] Soo M T, Cheong K Y and Noor A F M 2010 *Sens. Actuators B:-Chem.* **151** 39
[5] Zhang H, Guo H X, Zhang F Q, Pan X Y, Liu Y T, Gu Z Q, Ju A A and Ouyang X P 2022 *Chin. Phys. B* **31** 018501
[6] Soo M T, Cheong K Y and Noor A F M 2010 *Sens. Actuators B:-Chem.* **151** 39
[7] Yang S, Liang X, Cui J, Zheng Q, Sun J, Liu M, Zhang D, Feng H, Yu X, Xiang C, Li Y and Guo Q 2021 *J. Semiconduct.* **42** 082802
[8] Yu Q, Ali W, Cao S, Wang H, Lv H, Sun Y, Mo R, Wang Q, Mei B, Sun J, Zhang H, Tang M, Bai S, Zhang T, Bai Y and Zhang C 2022 *IEEE Trans. Nucl. Sci.* **69** 1127
[9] Emeliyanov V V, Vatuev A S and Useinov R G 2016 *IEEE Trans. Nucl. Sci.* **63** 2176
[10] Zhang T, Allard B and Bi J 2018 *Microelectron. Reliab.* **88–90** 631
[11] Takeyama A, Matsuda T, Yokoseki T, Mitomo S, Murata K, Makino T, Onoda S, Okubo S, Tanaka Y, Kandori M, Yoshie T, Hijikata Y and Ohshima T 2016 *Jpn. J. Appl Phys.* **55** 104101
[12] Zhang C X, Shen X, Zhang E X, Fleetwood D M, Schrimpf R D, Francis S A, Roy T, Dhar S, Ryu S H and Pantelides S T 2013 *IEEE Trans. Electron Devices* **60** 2361
[13] Samanta P and Mandal K C 2017 *J. Appl. Phys.* **121** 034501
[14] Hu D, Zhang J, Jia Y, Wu Y, Peng L and Tang Y 2018 *IEEE Trans. Electron. Devices* **65** 3719
[15] Liang X, Cui J, Zheng Q, Zhao J, Yu X, Sun J, Zhang D and Guo Q 2020 *Radiat. Effects Defects Solids* **175** 559
[16] Muthuseenu K, Barnaby H J, Galloway K F, Koziukov A E, Maksimenko T A, Vyrostkov M Y, Bu-Khasan K B, Kalashnikova A A and Privat A 2021 *IEEE Trans. Nucl. Sci.* **68** 611
[17] Abbate C, Busatto G, Tedesco D, Sanseverino A, Velardi F and Wyss J 2019 *IEEE Trans. Electron. Devices* **66** 4243
[18] Witulski A F, Ball D R, Galloway K F, Javanainen A, Lauenstein J M, Sternberg A L and Schrimpf R D 2018 *IEEE Trans. Nucl. Sci.* **65** 1951
[19] Wang Y, Lin M, Li X J, Wu X, Yang J Q, Bao M T, Yu C H and Cao F 2019 *IEEE Trans. Electron Devices* **66** 4264
[20] Shoji T, Nishida S, Hamada K and Tadano H 2015 *Microelectron. Reliab.* **55** 1517
[21] Titus J L, Wheatley C F, Burton D I, Mouret I, Allenspach M, Brews J, Schrimpf R, Galloway K and Pease R L 1995 *IEEE Trans. Nucl. Sci.* **42** 1928
[22] Li X, Jia Y, Zhou X, Zhao Y, Tang Y, Li Y, Liu G and Jia G 2020 *IEEE Electron. Device Lett.* **41** 216
[23] Scheick L Z and Selva L E 2007 *IEEE Trans. Nucl. Sci.* **54** 2568
[24] Kuboyama S, Mizuta E, Nakada Y and Shindou H 2019 *IEEE Trans. Nucl. Sci.* **66** 1710
[25] Gurimskaya Y, Dias de Almeida P, Fernandez Garcia M, Mateu Suau I, Moll M, Fretwurst E, Makarenko L and Pintilie I 2020 *Nucl. Instrum. Methods A* **958** 162221
[26] Busatto G, De Luca V, Iannuzzo F, Sanseverino A and Velardi F 2013 *IEEE Trans. Nucl. Sci.* **60** 3793
[27] Ikeda N, Kuboyama S, Satoh Y and Tamura T 2008 *IEEE Trans. Nucl. Sci.* **55** 3388
[28] Wan X, Zhou W S, Ren S, Liu D G, Xu J, Bo H L, Zhang E X, Schrimpf R D, Fleetwood D M and Ma T P 2015 *IEEE Trans. Nucl. Sci.* **62** 2830
[29] Ruff M, Mitlehner H and Helbig R 1994 *IEEE Trans. Electron. Devices* **41** 1040
[30] Roschke M and Schwierz F 2001 *IEEE Trans. Electron. Devices* **48** 1442
[31] Koh M, Ohdomari I, Igarashi K, Matsukawa T and Sawara S 1999 *J. Appl. Phys.* **85** 7814
[32] Van Overstraeten R and De Man H 1970 *Solid-State Electron.* **13** 583
[33] Haldar S, Maneesha, Khanna M K and Gupta R S 1994 *IEEE Trans. Electron. Devices* **41** 1674
[34] Shen P, Wang Y and Cao F 2022 *Chin. Phys. B* **31** 078501
[35] DasGupta S, Brock R, Kaplar R, Marinella M, Smith M and Atcitty S 2011 *Appl. Phys. Lett.* **99** 023503
[36] McWhorter P J and Winokur P S 1986 *Appl. Phys. Lett.* **48** 133
[37] Lenahan P M and Dressendorfer P V 1984 *J. Appl. Phys.* **55** 3495
[38] Akturk A, McGarrity J M, Potbhare S and Goldsman N 2012 *IEEE Trans. Nucl. Sci.* **59** 3258